INTERNATIONAL JOURNAL OF Experimental Pathology

Int. J. Exp. Path. (2014), 95, 101–119

ORIGINAL ARTICLE

Pathogenesis of percutaneous infection of goats with *Burkholderia pseudomallei*: clinical, pathologic, and immunological responses in chronic melioidosis

Carl Soffler*, Angela M. Bosco-Lauth†, Tawfik A. Aboellail*, Angela J. Marolf‡ and Richard A. Bowen†

**Department of Microbiology, Immunology, and Pathology, College of Veterinary Medicine and Biomedical Sciences, Colorado State University, Fort Collins, CO, USA, †Department of Biomedical Sciences, College of Veterinary Medicine and Biomedical Sciences, Colorado State University, Fort Collins, CO, USA and ‡Department of Environmental and Radiological Health Sciences, College of Veterinary Medicine and Biomedical Sciences, Colorado State University, Fort Collins, CO, USA*

INTERNATIONAL JOURNAL OF EXPERIMENTAL PATHOLOGY

doi: 10.1111/iep.12068

Received for publication: 10 May 2013
Accepted for publication: 26 November 2013

Correspondence:
Richard A. Bowen
Department of Biomedical Sciences
Colorado State University
1683 Campus Delivery
Fort Collins
CO 80523-1683
USA
Tel.: 970 491 5768
Fax: 970 491 3557
E-mail: richard.bowen@colostate.edu

SUMMARY

Melioidosis is a severe suppurative to granulomatous infection caused by *Burkholderia pseudomallei*. The disease is endemic to South-East Asia and Northern Australasia and is also of interest as a potential biological weapon. Natural infection can occur by percutaneous inoculation, inhalation or ingestion, but the relative importance of each route is unknown. Experimental infection models using mice have shown inhalation to be the most lethal route of exposure, but few studies have examined the pathogenesis of percutaneous infection despite its presumptive importance in natural disease. Caprine models are useful in the study of melioidosis because goats are susceptible to natural infection by *B. pseudomallei*, display similar epizootiology/epidemiology to that of humans within the endemic range and develop similar pathologic lesions. Percutaneous inoculation with 10^4 CFU of *B. pseudomallei* produced disease in all experimental animals with rapid dissemination to the lungs, spleen and kidneys. Initial fever was brief, but temperatures did not return to pre-infection levels until day 18, concurrent with a dramatic lymphocytosis and the transition to chronic disease. Distribution and appearance of gross pathologic and radiographic lesions in goats were similar to caprine aerosol infection and to reported human disease. The similarities seen despite different routes of infection suggest that host or bacterial factors may be more important than the route of infection in disease pathogenesis. The nature of melioidosis in goats makes it amenable for modelling additional risk factors to produce acute clinical disease, which is important to the study of human melioidosis.

Keywords
Burkholderia pseudomallei, goat, melioidosis, model, pathogenesis

Burkholderia pseudomallei has been recognized as the causative agent of melioidosis for just over a century in South-East Asia and northern Australasia (Whitmore & Krishnaswami 1912). Melioidosis has always been associated with significant morbidity and mortality but was considered rare for the 80 years following its discovery (Dance 1991). In the early 1990s, it was recognized as an emerging infectious disease, and the subsequent study of melioidosis and *B. pseudomallei* has grown exponentially over the last 20 years, particularly in the past 10 years after the designation of *B. pseudomallei* as a select agent by the United States Centers for Disease Control and Prevention because of its potential use in bioterrorism. However, the immediate significance of melioidosis as a naturally occurring disease is highlighted by its mortality rate, which has made it the third most common infectious cause of death in northeast Thailand (Limmathurotsakul *et al.* 2010).

The clinical epidemiology, presentations, diagnosis and treatment of melioidosis have been examined in many prospective and retrospective studies, which have led to a much greater understanding of human disease. However, the study of bacterial virulence factors, disease pathogenesis and the

development of novel preventative and therapeutic measures is fundamentally dependent on animal models of disease. Model development for the study of human disease has been pursued in the mouse (Leakey *et al.* 1998; Hoppe *et al.* 1999; Tan *et al.* 2008; Lever *et al.* 2009; Conejero *et al.* 2011; Goodyear *et al.* 2012), hamster (Dannenberg & Scott 1958; Brett *et al.* 1997), rat (Woods *et al.* 1993; van Schaik *et al.* 2008), pig (Najdenski *et al.* 2004), goat (Soffler *et al.* 2012), marmoset (Nelson *et al.* 2011), rhesus macaque and African green monkey (Yeager *et al.* 2012). The infrastructure and resources of biomedical research facilitates the use of murine models, which have dominated the study of melioidosis with only minor efforts being devoted to other species. However, the impetus for the development of novel models is to provide a comparative approach for the study of melioidosis as well as a much needed second animal model for the assessment of new therapeutic and preventative measures (Estes *et al.* 2010).

The success and utility of these models must be assessed in terms of the goals for the models and their limitations for the study of melioidosis. The majority of murine (Jeddeloh *et al.* 2003; Tan *et al.* 2008; Lever *et al.* 2009) and all recent non-human primate (NHP) models (Nelson *et al.* 2011; Yeager *et al.* 2012) have focused on acute inhalational disease. Much of this was born out of a focus on biodefense, although the importance of natural inhalational infection (Currie & Jacups 2003; Cheng *et al.* 2006; Chou *et al.* 2007) is supported to a similar extent as percutaneous infection by epidemiological data (Suputtamongkol *et al.* 1994, 1999; Phuong *et al.* 2008; Rammaert *et al.* 2011).

Partially by design and partially by inherent species susceptibility, many models reside on extremes of the spectrum of clinical disease. This can be useful for specific questions relating to the pathogenesis or assessing therapeutics, but it limits the ability to model the spectrum of human disease in a single species or add additional layers of complexity such as predisposing risk factors, which are present in 80% of melioidosis patients (Currie *et al.* 2010).

The final limitation to consider for the various model species is the natural occurrence of disease in wild or domestic populations. Natural infection in pigs is typically chronic or asymptomatic (discovered only at slaughter) and likely follows oral infection (Sutmoller *et al.* 1957; Laws & Hall 1963; Omar 1963; Thomas *et al.* 1981; Ketterer *et al.* 1986; Millan *et al.* 2007). Pigs have repeatedly been shown to be very resistant to experimental infection – even with immunosuppression (Stanton & Fletcher 1932; Thomas *et al.* 1990; Najdenski *et al.* 2004), such that they do not appear well suited for the study of melioidosis. Natural disease in several species of NHPs has been reported as well (Sprague & Neubauer 2004), but of the species used for experimental melioidosis models, disease (outside of zoological gardens) has only been reported in two rhesus macaques. Both animals exhibited chronic or reactivated latent disease, with diagnoses made 6 months and 10 years after acquisition (Kaufmann *et al.* 1970; Fritz *et al.* 1986). An outbreak in imported cynomolgus macaques with 13 cases has also been reported (Dance *et al.* 1992). While this species has been used in many aspects of biomedical research, it has not been investigated for the development of experimental melioidosis models.

The goat, as a naturally affected species, has a base of scientific literature describing the clinical presentation and pathology of melioidosis (Lewis & Olds 1952; Olds & Lewis 1954; Sutmoller *et al.* 1957; Omar 1963; Narita *et al.* 1982; Thomas *et al.* 1988; Van der Lugt & Henton 1995; Soffler *et al.* 2012), which compares well with human disease in terms of clinical presentation, epizootiology (Limmathurotsakul *et al.* 2012), organ distribution and histopathology (Piggott & Hochholzer 1970; Wong *et al.* 1995). While goats more frequently develop chronic disease, acute presentations are possible and therefore, goat models are likely amenable to the incorporation of risk factors to increase susceptibility or acute disease.

The goat model provides an opportunity to study the relative importance of the route of infection. Disease and outcome can be compared to natural presentations in both human and goat populations which have greater relevance because goats and humans are similarly exposed to environmental *B. pseudomallei*. The objective of this study was to create a non-fulminant, subacute to chronic percutaneous infection model of caprine melioidosis and compare its pathogenesis to natural disease and experimental aerosol infection (Soffler *et al.* 2012).

Materials and methods

Bacterial strain and culture methods

An Australian isolate of *B. pseudomallei* (Bp 4176/MSHR 511) (Pearson *et al.* 2007) was provided by Dr. Apichai Tuanyok. Bacteria for infection were grown in Muller–Hinton (MH) broth (M5887; Teknova, Hollister, CA, USA) at 37 °C in air with constant shaking at 250 rpm. Bacteria were harvested in mid-log phase growth, and, based on the OD 600, the culture was diluted in phosphate-buffered saline (PBS) to achieve a final concentration of 5×10^4 CFU/ml. A target dose of 1×10^4 CFU in 0.2 ml of PBS was selected based on pilot studies, which investigated a dose range of 8.2×10^2–10^6 (data not shown). The bacterial suspension used for infection was back titrated in duplicate on MH agar plates incubated at 37 °C in air.

In an effort to improve the sensitivity of blood culture from previous experiments (Soffler *et al.* 2012), a larger volume of blood (8.3 ml) was sterilely collected into 1.7 ml sodium polyanethol sulphonate (SPS, 0.35% in 0.85% sodium chloride) anti-coagulant (BD Vacutainer® 364960; Franklin Lakes, NJ, USA). Anti-coagulated blood was then mixed with 190 ml of molten (45 °C) MH agar and poured into three 15-cm Petri dishes for quantitative culture (Simpson *et al.* 1999). Once solidified, the plate was incubated at 37 °C in air. Plates were monitored for 7 days before being declared negative. Colonies seen on blood culture plates were subcultured onto selective media [MH agar with 4 mg/

l gentamicin (MH-gentamicin)] to verify gentamicin resistance and colony morphology consistent with *B. pseudomallei*. Nasal swabs, organ homogenates and abscess material were also cultured on MH-gentamicin plates at 37 °C in air and evaluated at 96, 48 and 48 h respectively.

Experimental animals

Seventeen adult Boer-cross goats were obtained through private sale for use in this experiment. Animals were obtained from herds that had no known history of and tested negative for caprine arthritis encephalitis and Johne's Disease (*Mycobacterium avium* subsp. *paratuberculosis*). Caseous lymphadenitis (CL) (*Corynebacterium pseudotuberculosis*) was present in some source flocks, and goats with visible lesions were excluded, as were the results from any goats with CL lesions found at necropsy.

Goats weighed 35–100 kg. There were fourteen females and three castrated males. Animals were housed in an animal biosafety level-3 facility for the duration of the experiment. They had *ad libitum* access to water and were fed a complete pelleted feed twice daily, supplemented with grass hay. Goats were acclimatized to the facility for approximately 1 week prior to infection. The bacterial suspension was inoculated (day 0) into the dermis (0.1 ml) and subcutaneous tissue (0.1 ml) overlying the caudolateral aspect of the brachium, for a total target dose of 10^4 colony-forming units (CFU).

Ethical Approval

This study was performed in strict accordance with the recommendations in the Guide for the Care and Use of Laboratory Animals of the National Institutes of Health and approved by the Animal Care and Use Committee of Colorado State University, and every effort was made to minimize suffering.

Clinical monitoring: haematology and clinical microbiology

Beginning on day −3, the goats' attitude, appetite and temperature were monitored daily for the duration of the experiment. Normal rectal temperature was defined as 38–40 °C. Four pre-infection complete blood counts (CBCs) (HemaTrue Hematology Analyzer; Heska Corporation, Loveland, CO, USA) were performed on each goat to establish baseline haematologic values. Postinfection (PI) CBCs were performed on days 1–7, 9, 11, 14, 18, 21, 25, 28, 32, 35, 39 and 42.

Previous blood collection for culture based on a set schedule yielded very few positive results (Soffler *et al.* 2012). Therefore, blood culture collection was targeted for only days 1–5 and then for any day where the rectal temperature was over 39 °C and had increased at least 0.6 °C over the temperature from the previous day. The collection site over the jugular vein was aseptically prepared with povidone iodine and ethyl alcohol, and blood was collected into a sterile tube prefilled with SPS anti-coagulant.

Nasal swabs of both nostrils were sampled daily for the duration of the experiment with a Dacron® fiber tipped plastic applicator swab (Cat. No. 14-959-90; Fisher HealthCare, Houston, TX, USA) and immediately streaked onto a MH-gentamicin agar plate.

Thoracic radiography

Two-view thoracic radiographs (right and left lateral) were taken under xylazine sedation for all goats prior to infection and on days 7, 14, 21, 28, 35 and 42. A ventrodorsal view was not included as previous experience showed it to be of limited diagnostic use. Radiographs of the extirpated lungs were also taken at the time of necropsy. Initial studies showed little to no radiographic change in the lungs on day 2; therefore, this necropsy time point was not aligned with radiography. Radiographs were taken using a MinXRay® 100HF (MinXray, Inc., Northbrook, IL USA) and Agfa® Computed Radiography (CR) 43 × 35 CR MD 4.0 General Cassettes (Agfa Healthcare NV, Mortsel, Belgium). The cassettes were processed with a CR 85-X digitizer, and the images were processed with NX software (Agfa Healthcare NV). All radiographs were read by AJM.

Euthanasia, necropsy, histology and organ burden

Humane euthanasia of goats with intravenous pentobarbital was planned for days 2, 7, 14, 21 and 42 PI. Five goats were assigned to the day 42 time point to ensure there were at least three goats surviving to that point. All other time points had three goats assigned. Necropsies were performed on all goats. Based on organ involvement detected in pilot studies, the following tissues were collected into 10% neutral-buffered formalin for histology: infection site (skin, subcutis and underlying muscle), prescapular lymph nodes (PSLN), retropharyngeal lymph node, tracheobronchial lymph node, mediastinal lymph node (MedLN), lungs, heart, spleen, liver, kidney, adrenal, thyroid, brain and mesenteric lymph node (MesLN). Samples were routinely embedded in paraffin, sectioned at 5 μm and stained with haematoxylin and eosin for microscopic evaluation. Selected tissues were also examined with Brown-Hopps staining when bacteria were visible with haematoxylin and eosin staining.

In organs with macroscopic abscesses, the abscesses were counted or estimated as a percentage of the total organ volume. Representative abscesses were cultured by impression smears on MH-gentamicin agar to confirm positive growth of *B. pseudomallei*. In the absence of macroscopic abscesses, samples of the following organs were aseptically collected to calculate the organ burden (CFU/g): lung (cranial, middle and caudal lobes of left and right lungs), spleen, liver, kidney, prescapular lymph node, MedLN and MesLN. Tenbroeck homogenizers were used to homogenize 0.5 g of each tissue sample in 2 ml PBS + 20% glycerol (limit of detection 25 CFU/g). Urine was also collected and cultured from each goat at the time of necropsy and cultured as neat urine and as a urine pellet (4 ml centrifuged at 7500 ***g*** for

10 min, limit of detection 5 CFU/ml). The homogenate or urine (100 μl) was plated in duplicate on MH-gentamicin agar, and the remaining sample was frozen at −80 °C. If the colony count was above the limit of quantitation (>300 colonies/plate), the frozen homogenate was thawed and serial log dilutions were plated in duplicate.

Cytokine measurement

Serum was collected for cytokine analysis prior to infection and on days 2, 7, 14, 21 and 42 PI. Postinfection sera were filtered using a low-protein-binding 0.2-μm syringe filter, cultured for sterility and frozen at −80 °C prior to analysis. Preinfection sera were centrifuged at 10,000 ***g*** for 10 min to remove platelets prior to analysis (filtration eliminated platelets in PI samples). Sera from goats infected in a previous experiment by intratracheal aerosol with the same target dose (Soffler *et al.* 2012) were similarly collected and stored for comparative analysis with samples from percutaneously infected goats. Analysis was performed using commercially available enzyme-linked immunosorbent assay (ELISA) kits for bovine CCL2 (VS0083B; Kingfisher Biotech, Inc., St. Paul, MN, USA), bovine IFNγ (VS0257B; Kingfisher Biotech, Inc.), bovine IL-10 (BV1495; TSZ ELISA, Framingham, MA, USA) and TGF-β1 (MB100B; R&D Systems, Minneapolis, MN, USA). Optimal dilution of sera for CCL2 and IFNγ was determined to be 1:8. Protocols were followed according to the manufacturer's instructions. Plates were read using a BioTek Synergy 2 multimode microplate reader and GEN5 software (BioTek Instruments, Inc., Winooski, VT, USA).

Data analysis

Summary measures of clinical data are reported as means and ranges. All statistical calculations were performed with SAS Version 9.3 (SAS Institute, Cary, NC, USA). The association between temperature, granulocyte count and lymphocyte count was analysed by the CORR Procedure using Pearson correlation. Temperature, granulocyte count, lymphocyte count and serum cytokine concentration data were analysed using the mixed procedure for repeated-measures ANOVA with an autocorrelation model (selected by AICC). Logarithmic (base 10) transformation was used for cytokine data to normalize data with outliers remaining after transformation excluded from analysis, which was only necessary for goat BpG48 in the analysis of IFNγ. Temperature, granulocyte count and lymphocyte count data were analysed for the effect of day, and cytokine data were analysed for the effect of day, route and route x day interaction. Results were considered significant with a $P < 0.05$.

Results

Bacterial dose and clinical monitoring

Infection was performed on three separate days. The back titration of the inocula ranged from 4.2×10^4 to 5.0×10^4 CFU/ml. The delivered dose to individual goats is reported in Table 1.

The mean body temperature for all goats prior to infection was 38.6 °C. Day 2 was the only day of the experiment where the mean temperature (40.1 °C) was in the febrile range, when 76% (13/17) of goats displayed fever. Of the four goats that were not febrile on day 2, two never became febrile and the others developed fevers on days 5 or 8. Two goats (BpG54 and 59) maintained temperatures well above pre-infection levels and often in the febrile range for the duration of the experiment (21 and 42 days respectively). While not meeting the definition of fever (>40 °C, other than day 2), mean temperatures were above the mean

Table 1 Goats infected with *B. pseudomallei* and status at euthanasia

Goat no.	Sex	Dose (CFU)	Day PI of necropsy	Status at euthanasia/death
BpG43	F	9.9×10^3	2	Febrile acute disease
BpG51	F	9.2×10^3	2	Febrile acute disease
BpG52	F	9.2×10^3	2	Febrile acute disease
BpG45	F	9.9×10^3	7	Subclinical subacute disease
BpG46	F	9.9×10^3	7	Subclinical subacute disease
BpG47	F	9.2×10^3	7	Febrile
BpG42	F	9.2×10^3	9*	Died, hypothermic, purulent nasal discharge, severe acute progressive disease
BpG50	F	9.9×10^3	14	Subclinical subacute disease
BpG44	F	9.9×10^3	14	Febrile subacute disease
BpG49	F	9.9×10^3	21	Subclinical chronic disease
BpG48	F	9.2×10^3	21	Subclinical chronic disease
BpG54	F	9.2×10^3	21	Febrile active disease
BpG55	F	8.5×10^3	42	Subclinical chronic disease
BpG56	MC	7.7×10^3	42	Subclinical chronic disease
BpG57	MC	8.5×10^3	42	Subclinical chronic active disease
BpG58	MC	8.5×10^3	42	Subclinical chronic active disease
BpG59	F	8.5×10^3	42	Subclinical chronic active disease

F, female; MC, male castrated.
*Died 5 days prior to intended date of euthanasia.

pre-infection temperature by 0.7 to 1.5 °C from days 1 through 17, which were all significantly higher than day 0 ($P \leq 0.0005$). Day 18 was the first day that the mean temperature was not significantly different from day 0 ($P = 0.14$). The mean temperature was significantly different for only 7 of the remaining 24 days, indicating an overall return to pre-infection levels. The variability of temperatures of individual goats as well as the mean temperatures over the duration of the experiment is shown in Figure 1.

Despite fevers (up to 41.4 °C), lethargy or decreased appetite was rarely observed. Two goats were mild to moderately lethargic on day 2 in association with fever. Moderate lethargy and inappetence were first noted on day 8 in BpG42, which rapidly deteriorated to severe lethargy, obtundation and death on day 9 (before euthanasia could be performed). This goat was the thinnest of all the animals and never developed a fever.

The most frequent clinical sign recognized was swelling at the site of infection and enlargement of the ipsilateral prescapular lymph node. The subcutaneous swelling organized into abscesses that ruptured in 80% (8/10) of goats that survived through day 14 (no abscess ruptured in any goat prior to day 14). Lameness was only noted in one goat in association with an injection site abscess that was quite large, but did not rupture. Cough was intermittently noted in two goats (BpG54 and 59). Significant nasal discharge was rarely observed, with one goat developing purulent discharge 3 days prior to death (BpG42) and another (BpG54) briefly developing haemorrhagic discharge on day 16.

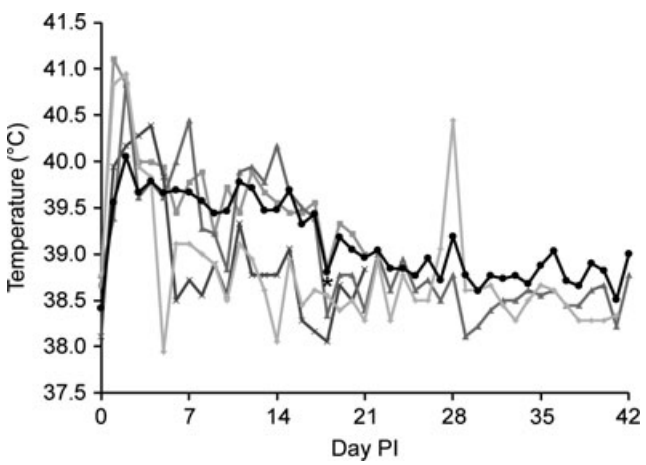

Figure 1 Mean temperatures and selected representative goats. Peaks in temperature were typically seen on days 1 and 2, although later peaks are possible as seen in BpG49 on day 4. Day 18 was the first day that the mean temperature was not significantly different from day 0 (*$P = 0.14$). The peak in BpG57 on day 28 highlights the chronic active nature of disease at later time points. Mean (●), BpG48 (■), BpG49 (×), BpG56 (▲), BpG57 (□).

Haematology

Pre-infection haematology was generally unremarkable in regard to red cell parameters, and no remarkable changes were observed during the course of infection. White cell parameters were more variable during the pre-infection sampling, which were attributed to a cortisol response from handling during the acclimatization period. The mean pre-infection white blood cell counts for all goats over all independent samples were as follows: total white blood cells 11.9×10^3 cells/μl (range 4.9–26.3 $\times 10^3$ cells/μl, reference range 4–13 $\times 10^3$ cells/μl); lymphocytes 4.8×10^3 cells/μl (range 2.4–7.7 $\times 10^3$ cells/μl, reference range 2–9 $\times 10^3$ cells/μl); monocytes 0.8×10^3 cells/μl (range 0.2–1.6 $\times 10^3$ cells/μl, reference range 0–1 $\times 10^3$ cells/μl); and granulocytes 6.4×10^3 cells/μl (range 1.6–21.2 $\times 10^3$ cells/μl, reference range 1.2–7.2 $\times 10^3$ cells/μl). While some leucocyte counts were elevated at individual time points, only one goat (BpG42) maintained mildly elevated granulocyte count for all samples. All other goats and leucocyte parameters measured within the reference range for at least one pre-infection time point.

The only cell types with a notable PI response were granulocytes and lymphocytes (see Figure 2). The mean granulocyte counts showed significant increases on days 1 and 2 ($P < 0.0001$), and remained significantly elevated above day 0 through day 35 ($P < 0.05$) and above the reference range through the end of the study. The peak on day 2 was followed by a more gradual but higher peak on day 18, returning to pre-infection levels on days 39 and 42 ($P = 0.055$ and $P = 0.10$ respectively). The granulocyte count was moderately positively correlated with temperature ($r = 0.41$, $P < 0.0001$).

The mean lymphocyte count was generally unremarkable for the first 14 days of the experiment. Significant increases above day 0 but within the normal range were observed on days 11 and 14 ($P = 0.048$ and $P = 0.009$ respectively). The greatest increase in lymphocyte count and above the normal range was seen on day 18 ($P < 0.0001$), which peaked on day 28 ($P < 0.0001$) before returning to pre-infection levels and the normal range on day 35 ($P = 0.20$). The lymphocyte count showed a weak, but significant negative correlation with temperature ($r = -0.16$, $P = 0.027$).

Clinical microbiology

Nasal swabs were positive for *B. pseudomallei* in 35% (6/17) of goats over the course of the entire study. Of the six goats that cultured positive, only three were noted to have grossly evident nasal discharge, which aligned with the timing of the positive cultures in two goats. Four of the six goats to have positive nasal cultures were in the group euthanized on day 42, but otherwise there was no pattern of timing or distribution of cultures, which ranged from only a single positive culture, to intermittent shedding, or positive culture for nearly all of the latter 3 weeks of the study. Thick nasal discharge with heavy growth of *B. pseudomallei*

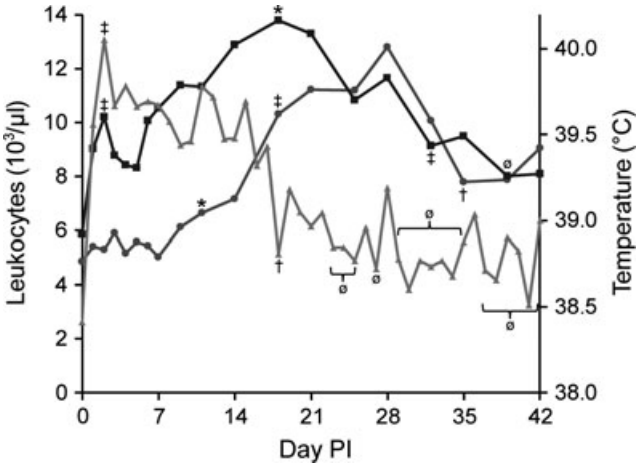

Figure 2 Mean granulocyte count, lymphocyte count and temperature. Granulocytes (■) showed an initial peak on day 2 and then on day 18 before a significant decrease on day 32 and a return to pre-infection levels on day 39. Lymphocytes (●) first increase over pre-infection levels on day 11, with a significant increase out of the normal range on day 18, which is associated with a significant decrease in temperature (▲) to pre-infection levels. Lymphocytes significantly decrease to pre-infection levels on day 32. (‡) Different than previous measure and pre-infection, (†) different than previous measure but no different than pre-infection, (*) different than pre-infection, (ø) not different than previous measure or pre-infection, significance $P < 0.05$.

was associated with terminal disease in goat BpG42, but not in any other goat. Growth from the nasal swabs was typically light to moderate.

Quantitative blood culture was negative for *B. pseudomallei* for all goats at all time points.

Thoracic radiography

Pre-infection radiographs for all goats were within normal limits (Figure S1) except for BpG51, which appeared to have chronic changes from a previous episode of pneumonia (no clinical or haematologic finding supported active disease prior to infection). Pulmonary disease was radiographically evident in 64% (9/14) goats by day 7. Changes ranged from a mild local bronchointerstitial pattern in the dorsal aspect of the caudal lung lobes to moderate diffuse bronchointerstitial infiltrates with or without nodular opacities (4–6 mm), suggesting small abscesses or pyogranulomas associated with pneumonia (Figure 3a). Extirpated lung radiographs of the goats euthanized on day 7 showed the same bronchointerstitial infiltrates but revealed more numerous small nodules throughout the lung lobes (which was typical for all extirpated radiographs compared to *in vivo* imaging). BpG42 has the worst changes with interstitial coalescing to alveolar infiltrates and 1- to 2-cm nodules in the dorsal aspect of the caudal lung lobes, which progressed to diffuse nodular interstitial to alveolar infiltrates in all lung lobes at the time of death on day 9. Radiographic evidence of pneumonia was present in 90% (9/10) goats by day 14. The changes were generally progressive, with increasing patchy (more caudodorsally) to diffuse bronchointerstitial infiltrates that follow the caudal bronchi seen in goats with radiographic changes. Bronchointerstitial changes range from mild to severe, with occasional peribronchial cuffing and alveolar infiltrates. Multiple ill-defined, variably sized (5–11 mm) soft tissue opaque nodules were present in 67% (6/9) goats with radiographic evidence of pulmonary disease, which were very numerous in individual goats (Figure 3b). All eight goats had radiographic evidence of disease on day 21, with half of the goats having static lesions. Progression was typified by more widespread and/or worsening bronchointerstitial and alveolar infiltrates, more numerous and larger nodules (3–20 mm) (Figure 3c,e). Nodules were observed in 75% (6/8) goats. The remaining five goats had unchanged lesions on days 28 and 35 with the exception of BpG56, where nodular lesions were less distinct than day 21. By day 42, the nodular lesions in BpG55, 56 and 59 were distinctly smaller (Figure 3d). Worsening bronchointerstitial and alveolar infiltrates were seen in two goats, while no evidence of progression was seen in the remaining two goats. Nodular lesions were visible in all extirpated lungs, with a 20 mm cavitated lesion observed in BpG59 (Figure 3f).

Gross pathology

Organ involvement for individual goats is summarized in Table 2. The only acute lesion observed on day 2 was subcutaneous oedema at the injection site. Lesions of chronic pneumonia were observed in BpG51, corresponding to the reported radiographic findings, along with an abscessed mediastinal LN; these changes were judged to not be related to the experimental infection.

By day 7, discrete, 2–4 mm, cream coloured abscesses with caseopurulent centres within the dermis and/or subcutis at the site of infection and ipsilateral prescapular LN abscesses were present at the site of infection and in the ipsilateral prescapular lymph node. Abscesses were additionally seen in the lungs, spleen and kidney. In the lungs, the abscesses were surrounded by a dark red rim of consolidated parenchyma. Renal lesions appeared as 3- to 4-mm nodules protruding above the surface, which when cut revealed cream coloured, linear and variably sized abscesses originating in the cortex and expanding towards the medulla, with the adjacent parenchyma discoloured tan.

One thin goat (BpG42) was the only goat to die (day 9) from experimental infection. Apart from a small abscess observed at the site of infection, there was minimal oedema of surrounding dermis and subcutis. Internal gross lesions were consistent with fulminant disease, with oedematous connective tissue throughout the body, subpleural oedema, fibrinous pleural adhesions and serosanguinous hydrothorax. The lungs were consolidated and filled with small, multifocally extensive (miliary) abscesses (Figure 4a). The only other organ with a visible abscess was the kidney, which was very small (1 mm surface diameter) but had the

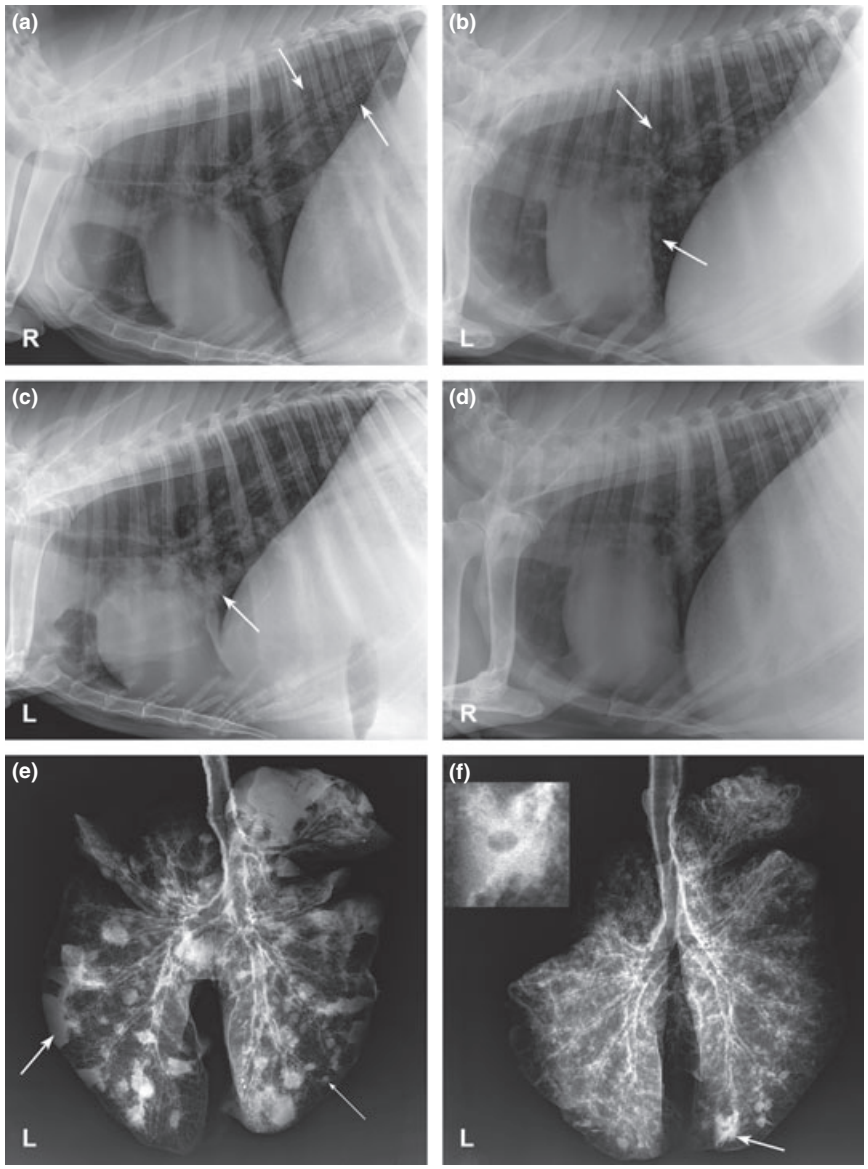

Figure 3 Thoracic and extirpated lung radiographs of goats infected percutaneously with *B. pseudomallei*. (a) BpG47, day 7, right lateral thorax, moderate bronchointerstitial infiltrates and small ill-defined nodular infiltrates in the dorsocaudal and cranioventral lung lobes (arrows). (b) BpG59, day 14, left lateral thorax, moderate-severe bronchointerstitial infiltrates and numerous nodules (5–11 mm) throughout the pulmonary parenchyma (arrows). (c) BpG54, day 21, left lateral thorax, moderate diffuse bronchointerstitial infiltrates, patchy alveolar infiltrates in the mid-caudal lung lobes, bronchoalveolar infiltrates in cranioventral lung lobes (arrow) and numerous nodular opacities (6–16 mm) throughout the pulmonary parenchyma. (d) BpG59, day 42, progression of the bronchointerstitial infiltrates with several poorly defined opacities/alveolar infiltrates within the lungs, although nodules are less defined than on day 14. (e) BpG54, day 21, extirpated lungs, numerous nodules (thin arrow) and several focal areas of consolidation (arrow) throughout the parenchyma with a dense bronchial pattern diffusely. (f) BpG59, day 42, extirpated lungs, severe diffuse bronchointerstitial pattern with a large 2 cm cavitated nodule (inset) in the right caudal lung lobe (arrow) with several other nodules in the remaining lungs.

characteristic linear structure when cut. Lymphadenomegaly was observed in the mediastinal and mesenteric LNs.

Lesions at day 14 and beyond were variable among goats, but affected similar organs as seen on day 7. Additional lesions observed included pulmonary fibrous adhesions (Figure 4b arrow), abscesses extending down into the muscle underlying the injection site, mammary abscess, and tracheobronchial and retropharyngeal lymphadenomegaly and abscessation. The nasal turbinates from BpG59 were filled with mucopurulent exudate. A single 2-mm liver abscess was noted in one goat (BpG48). The sublumbar lymph nodes were grossly enlarged, discoloured black by draining haemorrhage and contained small abscesses in one goat (BpG58).

Table 2 Summary of organ burdens

Goat No.	Day	Injection site	PSLN	RPLN	Lung	MedLN	Liver	Spleen	Kidney	MesLN	Urine
BpG43	2	<LOD	2.5×10^5	<LOD	<LOD	<LOD	<LOD	<LOD	<LOD	<LOD	<LOD
BpG51	2	<LOD	3.6×10^5	<LOD	25	<LOD	<LOD	<LOD	<LOD	<LOD	<LOD
BpG52	2	3.0×10^3	2.4×10^4	<LOD	50	<LOD	<LOD	25	<LOD	<LOD	<LOD
BpG53	2	<LOD	<LOD	<LOD	<LOD	<LOD	<LOD	<LOD	<LOD	<LOD	<LOD
BpG45	7	2.3×10^2	+	<LOD	+	<LOD	<LOD	<LOD	<LOD	<LOD	<LOD
BpG46	7	+	+	<LOD	+	<LOD	<LOD	<LOD	+	<LOD	<LOD
BpG47	7	+	+	<LOD	+	1.0×10^2	<LOD	+	<LOD	<LOD	<LOD
BpG42	9	+	6.3×10^3	1.3×10^3	+	1.7×10^3	3.0×10^4	2.8×10^5	+	1.8×10^2	3.0×10^5
BpG44	14	+	3.8×10^2	<LOD	+	25	<LOD	<LOD	+	<LOD	<LOD
BpG50	14	+	<LOD	<LOD	50	<LOD	<LOD	5.5×10^2	<LOD	<LOD	<LOD
BpG48	21	+	+	<LOD	+	+	+	+	<LOD	<LOD	<LOD
BpG49	21	+	+	<LOD	+	<LOD	<LOD	<LOD	<LOD	<LOD	<LOD
BpG54	21	+	+	<LOD	+	+	<LOD	+	+	<LOD	10
BpG55	41	+	+	<LOD	+	75	<LOD	+	+	<LOD	<LOD
BpG56	42	+	+	<LOD	+	+	<LOD	+	+	25	5.5
BpG57	41	+	+	<LOD	+	<LOD	<LOD	+	<LOD	<LOD	<LOD
BpG58	42	–	+	25	+	<LOD	<LOD	+	+	<LOD	1.0×10^3
BpG59	42	+	+	+	+	+	<LOD	+	+	<LOD	5.9×10^2

PSLN, prescapular lymph node; RPLN, retropharyngeal lymph node; MedLN, mediastinal lymph node; MesLN, mesenteric lymph node; <LOD, below limit of detection; +, growth of *B. pseudomallei* from grossly observed abscess; –, no growth of *B. pseudomallei* from grossly observed abscess.
Unit for tissue culture is CFU/g. Unit for urine culture is CFU/ml.

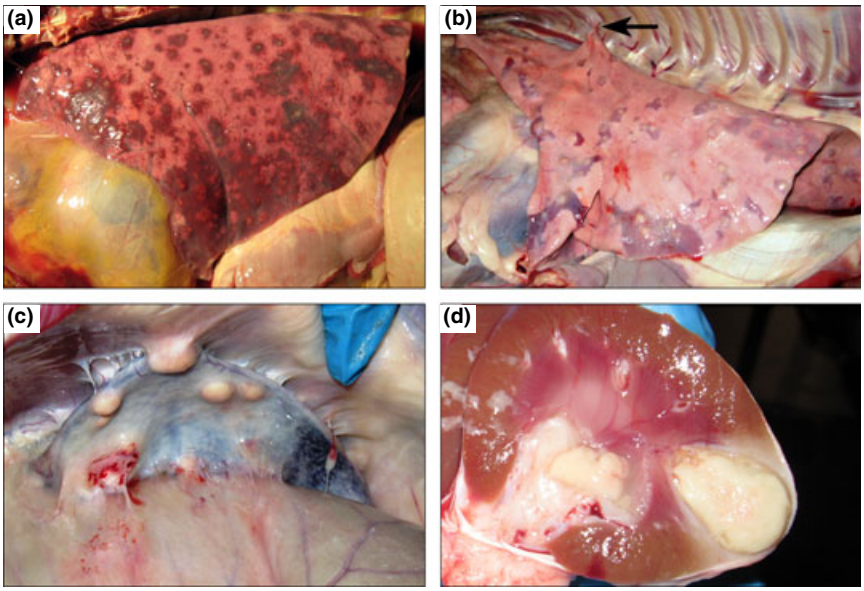

Figure 4 Gross lesions of caprine melioidosis. (a) Lung, numerous, multifocal, discrete to coalescing abscesses/pyogranulomas associated with extensive consolidation and haemorrhage; (b) lung, typical subpleural targetoid pyogranulomas with tan purulent centres and consolidated hyperaemic rims that are rarely associated with fibrous pleural adhesions; (c) spleen, multiple, large pyogranulomas with adhesions of the splenic capsule to the peritoneum; (d) kidney, multifocally extensive and coalescing pyogranulomas spanning from cortex to medulla.

Abscesses were typically more numerous and larger at later time points, particularly for the prescapular lymph node, spleen and kidneys (Figure 4c,d). Splenomegaly was often present by day 42 with numerous (30–40) and large (15 mm) pyogranulomas effacing nearly half of the organ and adhering the spleen to the peritoneum/body wall (Figure 4c). Pulmonary abscesses were typically small (~5 mm), although individual goats had lesions up to 20 mm in diameter. Lung lesions were concentrated in the caudal lung lobes, which was especially true for the larger lesions. The cavitary lesion seen radiographically in BpG59 (Figure 3f) corresponded with a larger abscess. On cut surface, the cavity consisted of an empty necrotic centre encased by an irregular wall that was 1–2 mm thick. After formalin fixation, several smaller abscesses in this goat were also noted to have very small (1 mm diameter) cavities.

Bacterial organ burden

The bacterial organ burden for all goats is summarized in Table 2. Positive cultures were most common from the lungs and ipsilateral prescapular LN (94%), injection site (88%), spleen (65%), and kidney and mediastinal LN (47%).

Burkholderia pseudomallei was isolated from all sampled abscesses, with the notable exception of the abscess at the site of infection in BpG58. Positive growth was generally restricted to areas of gross lesions with the exceptions of lymph nodes, which were often positive with no gross changes or only enlargement. Multiple organs from BpG42 also cultured positive, with relatively high levels of growth, which appeared to be associated with fatal fulminant septic shock. Urine culture at necropsy was positive in five of 17 goats, with one positive culture coming from the pellet only.

Histopathology

Skin/infection site. Typical lesions at day 2 included lymphangiectasia and lymphoedema, perivascular fibrin deposition, and microscopic haemorrhages in the dermis and panniculus. Predominantly neutrophilic, pleocellular exudate (Figure 5a 'N') variably obliterated adnexa, cuffed and tracked along inflamed vessels and peripheral nerves into skeletal muscles along interstitial planes. Affected vessels were segmentally to circumferentially obliterated by fibrinoid necrosis and/or leucocytes. The lining endothelial cells were hypertrophic, and the lumina were occluded by fibrinocellular thrombi with neutrophilic margination. By day 7, the vasculitis was less prominent, and the previous changes had progressed to multifocal and coalescing pyogranulomas. Necrotic epidermis clefted from the underlying dermis (Figure 5a 'C') and the inflamed surface was largely replaced by granulation tissue. On days 14–42, the epidermis was occasionally infarcted leaving a wide ulcer covered by granulation tissue, which incorporated numerous intact and degenerate neutrophils and mixed bacteria. The dermal and subcutaneous inflammation became predominantly lymphocytic with central mineralization of the older granulomas. Cicatricial dermal fibrosis and alopecia developed in the goats where the infection site abscess/pyogranulomas drained. Muscular interstitial septa were expanded by

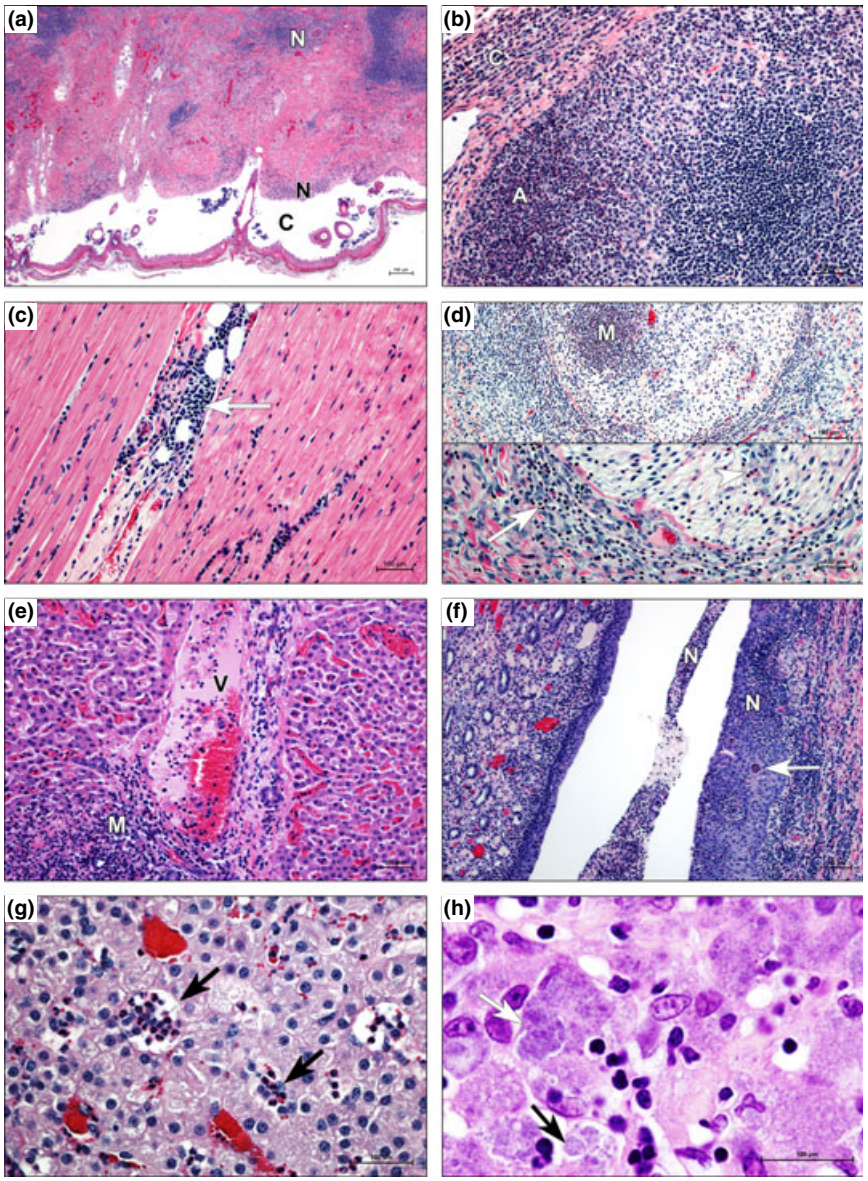

Figure 5 Extrapulmonary histologic lesions of percutaneous caprine melioidosis. (a) Skin, multifocally extensive neutrophilic infiltrates (N) expand the deep dermis surrounding vessels and adnexa with subepidermal clefting (C); (b) prescapular LN, capsulitis (C) and early subcapsular abscess (A) involving the subjacent lymphoid follicle; (c) heart, lymphoplasmacytic interstitial myocarditis (arrow) infiltrating along tissue planes; (d) spleen, upper panel: neural microabscesses (M) in a larger splenic nerve, lower panel: mild suppurative perineuritis (arrow) and minimal numbers of neutrophils infiltrating (arrow head) a smaller splenic nerve; (e) liver, vasocentric portal microabscess (M) obliterating the lower pole of a portal vein (V); (f) kidney, suppurative pyelonephritis with degenerate neutrophils (N) filling the lumen, infiltrating the pelvic lining forming a mucosal abscess (arrow), and invading the suburothelial stroma; (g) adrenal, microabscesses (arrows) with lytic necrosis are scattered within the zonae fasciculata and reticularis; and (h) mesenteric LN, phagocytically active macrophages with abundant intrahistiocytic (white arrow) and extracellular (black arrow) coccobacilli. Haematoxylin and eosin staining.

mature fibrous connective tissue that isolated small groups of hyalinized and atrophic muscle fibres.

Prescapular LN. Ipsilateral to Infection Site: Acute lesions manifested as variably severe suppurative capsulitis (Figure 5b 'C') that involved capsular vessels, which occasionally resulted in perivascular haemorrhage. Vasculitis was most prominent on day 2 and was not observed after day 7 PI. The subcapsular sinuses occasionally contained small numbers of macrophages with intracytoplasmic bacteria. Multifocal discrete to coalescing pyogranulomas formed first in the subcapsular area (Figure 5b 'A') and progressed as suppurative inflammation tracking along trabeculae, inciting fibrinoid necrotizing vasculitis of the deeper vessels with

extension of the inflammation to the hilus. The neutrophilic centres of acute pyogranulomas were gradually filled and replaced by macrophages/multinucleate cells on or after day 14. The histiocytic layer encroached on those centres showing increasingly prominent phagocytic activity as the lesions regressed. The capsule in the chronic stage was markedly thickened (10 times normal) by mature fibrous connective tissue and rare aggregates of lymphocytes. The capsular vessels were also enlarged due to medial hypertrophy. Lymphoid hyperplasia was marked in the cortex, and in rare instances, lymphocytes were intermixed with areas of extramedullary haematopoiesis. Lesions in the ipsilateral node were seen in all goats. *Contralateral to Infection Site*: Nonspecific changes of mild-to-moderate oedema, lymphoid hyperplasia and sinus histiocytosis were often present.

Heart. Lesions were observed in 94% (16/17) goats, which ranged from minimal to mild, focal to multifocal and random, lymphocytic to lymphoplasmacytic myocarditis, with rare (one goat) neutrophilic infiltrates. The interstitium was typically expanded by perivascular infiltrates of lymphoplasmacytes that followed along tissue planes (Figure 5c arrow). The infiltrates occasionally surrounded individual degenerate cardiomyocytes, which had fragmentation of their sarcoplasm, hyalinization and loss of cross-striations. Moderate lesions had peripheral microvascular haemorrhages and oedema. Occasional Purkinje fibres were also degenerate and inflamed. Slightly increased satellite cell activity was observed along with rowing of nuclei, indicative of a regenerative attempt.

Spleen. Early changes consisted of moderate-to-severe congestion and increased numbers of neutrophils, which rarely formed prominent perifollicular rings. Mild extramedullary haematopoiesis was rarely noted. Progression typically involved the development of suppurative capsulitis with vascularized granulation tissue, leukocytoclastic phlebitis and mesothelial cell hypertrophy. As typical pyogranulomas developed, capsular thickening (5–20× normal) and multifocal haemorrhages were observed. Older pyogranulomas were devoid of vasculitis with encroachment of the outer histiocytic layer upon neutrophilic centres. The exception to this was BpG59 which had extensive pyogranulomas involving most of the spleen. These pyogranulomas were noted to extend to the splenic parenchyma via necrotic trabeculae, which contained similar pyogranulomas. Vascular changes were still prominent at day 42 and included: necrotic vessels at the centre of pyogranulomas with capsular vessels showing medial hypertrophy and intimal hyperplasia. Additionally, several nerves at the periphery of resolving granulomas were surrounded by lymphoplasmacytic inflammation (Figure 5d arrow) and occasionally infiltrated by neutrophilic exudate and microabscesses (Figure 5d arrowhead and 'M').

Liver. Lesions were very common, 94% (16/17) of goats, but typically mild with no apparent association between time point and severity. Minimal to mild random hepatitis with piecemeal necrosis, lymphoplasmacytic aggregates and neutrophil infiltrates were seen at all time points. Moderate lesions occasionally localized around portal areas and tended to be more neutrophilic (microscopic abscesses) (Figure 5e 'M'). Rarely, the central veins were markedly ectatic and congested. The endothelial lining of those vessels were disrupted by small neutrophil infiltrates extending into adjacent foci of necrotic hepatocytes. Occasional necrogranulomas were also seen scattered within the parenchyma. Microscopic haemorrhage was observed in two goats, associated with the capsule and minimal aggregates of neutrophils or in areas of sinusoidal oedema.

Kidney. Varying degrees of histologic lesions were observed in 76% (13/17) of goats, with 61% (8/13) of lesions involving culture positive pyogranulomas. Inflammation began in cortical glomeruli, which appeared hypercellular due to neutrophilic infiltrates, and then involved the tubules and intervening interstitium, expanding towards the capsule causing suppurative capsulitis. Affected tubules showed attenuation of the lining epithelium to low cuboidal or squamoid cells with luminal proteinosis and neutrophils. Suppurative tubulointerstitial nephritis progressed in the inner medulla towards the renal pelvis accompanied with marked ectasia of the distal tubules and collecting ducts. Alongside the inflammation, vascular lesions commonly included leukocytoclastic vasculitis, fibrinocellular thrombi and vascular necrosis with severe congestion, perivascular fibrin deposition and haemorrhage. Suppurative inflammation eroded into the renal pelvis in 50% (4/8) goats with renal pyogranulomas. The lumina were filled with large numbers of intact and degenerate neutrophils that also invaded the suburothelial stroma (Figure 5f 'N') with occasional mucosal abscesses (Figure 5f arrow). These characteristic linear infiltrates spanned the renal parenchyma, maturing into typical chronic pyogranulomas. However, lesions were still active at day 42 with vasculitis, suppurative pyelonephritis and visible colonies of coccobacilli.

Adrenal. Minimal changes were observed in four goats independent of time point, with only three showing a suppurative component. The mildest change was a slight increase in fluid at the corticomedullary junction, which was associated with congestion and increased neutrophils within cortical capillaries. Blood sinuses were occasionally occluded by fibrin thrombi with minimal lytic necrosis. Microabscesses were rarely observed in the inner cortex (Figure 5g arrows).

Retropharyngeal LN. Changes variably consisted of hyperplasia, oedema, sinus histiocytosis and rare hemosiderosis. A smaller pyogranuloma was present in BpG59.

Mesenteric LN. Mild-to-moderate suppurative capsulitis and pericapsulitis were observed in association with neutrophilia in the medullary sinuses in BpG48. BpG42 had unique lesions of ectatic medullary sinuses due to oedema and small haemorrhages. Additionally, the node contained

many phagocytically active macrophages with intra- and extra-cytoplasmic gram-negative bacteria (white and black arrows, respectively, Figure 5h), small numbers of neutrophils, hemosiderin laden macrophages and plasma cells. Changes in other goats consisted of variable hyperplasia, oedema, sinus histiocytosis and rare hemosiderosis.

Mammary gland. Involuting or dry mammary glands without significant inflammation were present in all female goats except BpG48, which had a large pyogranuloma. Squamous metaplasia was present in the lining epithelium of a large duct with massive luminal aggregates of degenerate neutrophils intermixed with large colonies of coccobacilli and moderate numbers of phagocytically active macrophages. The lining epithelium contained small mucosal abscesses with a cleft that separated keratin into the lumen.

Sublumbar LN. The sublumbar LNs were only noted to be grossly abnormal in BpG58. Nodes were enlarged 5× normal size with focal resolving pyogranulomas and marked expansion of subcapsular, interfollicular and medullary sinuses with haemorrhage and erythrophagocytosis in the midst of marked follicular hyperplasia, chronic active trabeculitis and variably severe capsulitis.

Nasal turbinates. Neutrophils filled the lumen of eroded sinuses and lumina of several glands, which were slightly hyperplastic along with goblet cells of the respiratory epithelium in goat BpG59 (a chronic shedder). Occasional necrosis was seen in the boney trabeculae with multifocally increased osteoblastic activity and stromal inflammation.

Trachea. At day 2, lymphoplasmacytic tracheitis was characterized by a submucosal band of lymphoplasmacytes (Figure 6a 'L'), variable deciliation of the lining epithelium, transcytosis (Figure 6a arrows) and luminal aggregates of neutrophils. The findings on day 7 ranged from histologically normal or static lymphoplasmacytic tracheitis to progressive erosive tracheitis with the formation of mucosal abscesses. A neutrophilic component to the tracheitis was observed in four of five goats on days 14 and 21, with scattered foci of apoptosis/necrosis scattered throughout the mucosa. On day 42, only minimal to mild lymphoplasmacytic tracheitis was observed. Tracheal lesions were very common, being found in 88% (15/17) of goats.

Lung. Initial mild-to-moderate changes included oedema, atelectasis and congestion of interlobular vessels with perivascular neutrophil infiltrates spilling into alveolar spaces with small clusters of macrophages. More advanced changes seen on day 2 included terminal airways and mainstem bronchi filled by luminal aggregates of neutrophils and variable necrosis of the lining epithelium (Figure 6b arrow). Severely affected lobules were largely collapsed and infiltrated by a more mixed inflammatory infiltrate. On day 7, alveolar spaces were filled with fibrinocellular exudate, and scattered alveoli were lined by type 2 pneumocytes. Interlobular septa and connected pleurae were expanded by oedema, inflammatory pleocellular infiltrates and occasionally associated with granulation tissue or mature fibrous connective tissue on or after day 21. Vasocentric abscesses (Figure 6c 'N') surrounded necrotic vessels (Figure 6c 'V'), which were associated with microscopic haemorrhage (Figure 6d 'H'), oedema (Figure 6d 'E') and thrombosis (Figure 6e 'T'). Leukocytoclastic vasculitis was randomly distributed throughout affected lobules, although more evident in medium-sized arterioles. Occasional vessels showed intimal proliferation and scattered mitotic figures (Figure 6f arrowhead) in hyperplastic endothelial cells. By day 14, lesions were still active with necrosuppurative bronchiolitis to fibrinopurulent bronchopneumonia and vasculitis. As the lesions progressed, fibrosing bronchointerstitial pneumonia was increasingly evident. After day 21, bronchiolar epithelium showed marked hyperplasia, narrowed lumina and replacement of peribronchiolar parenchyma by granulation tissue. Chronic active bronchointerstitial pneumonia with fibrosis (Figure 6g 'F'), suppurative infiltrates (Figure 6g arrow) and oedema (Figure 6g 'E') was present in some goats as early as day 14 and nearly all goats from days 21 to 42, with vasculitis becoming less common although still observed in areas of active disease. Mature pyogranulomas were the most common lesion, having the typical structure (as in other tissues) from inside out as follows: variably thick liquefied centres with multifocal groups comprised of intact and degenerate neutrophils; a layer of epithelioid macrophages 5–10 cells thick with the innermost layer showing increased phagocytic activity and occasional bi- to multinucleate giant cells; a layer of lymphoplasmacytes arranged in concentric rows intermixed with fewer macrophages and neutrophils; and an outer encasement of granulation tissue that compresses the surrounding parenchyma. Resolving pyogranulomas showed thick capsules (Figure 6h 'C'), increasing numbers of macrophages (Figure 6h 'M') and giant cells (Figure 6h arrow), a thick mantle of lymphocytes (Figure 6h 'L') and diminished liquefied centres (Figure 6h 'N'). Cavitary lesions appeared to be a result of the liquefactive centre retracting away from the surrounding mantle.

BpG42 developed fatal disease on day 9, which was associated with an overwhelming severe pneumonia. Abscesses were surrounded by highly vascularized granulation tissue and markedly congested parenchyma with multifocal areas of haemorrhage, and many vessels occluded by fibrinocellular thrombi. Abscesses multifocally eroded into vessels, interlobular septa and terminal bronchioles. Medium-sized veins and arteries and adjacent airways were largely replaced by dense aggregates of intact and degenerate neutrophils. Necrotic walls of affected vessels were segmentally to circumferentially obliterated by leucocytes leading to the formation of vasocentric lesions. Walls of affected arteries had occasional outpouchings (microscopic aneurysms) with medial haemorrhage and intimal proliferation. Many macrophages and lesser numbers of neutrophils were studded with bacteria, which appeared as intensely basophilic bodies.

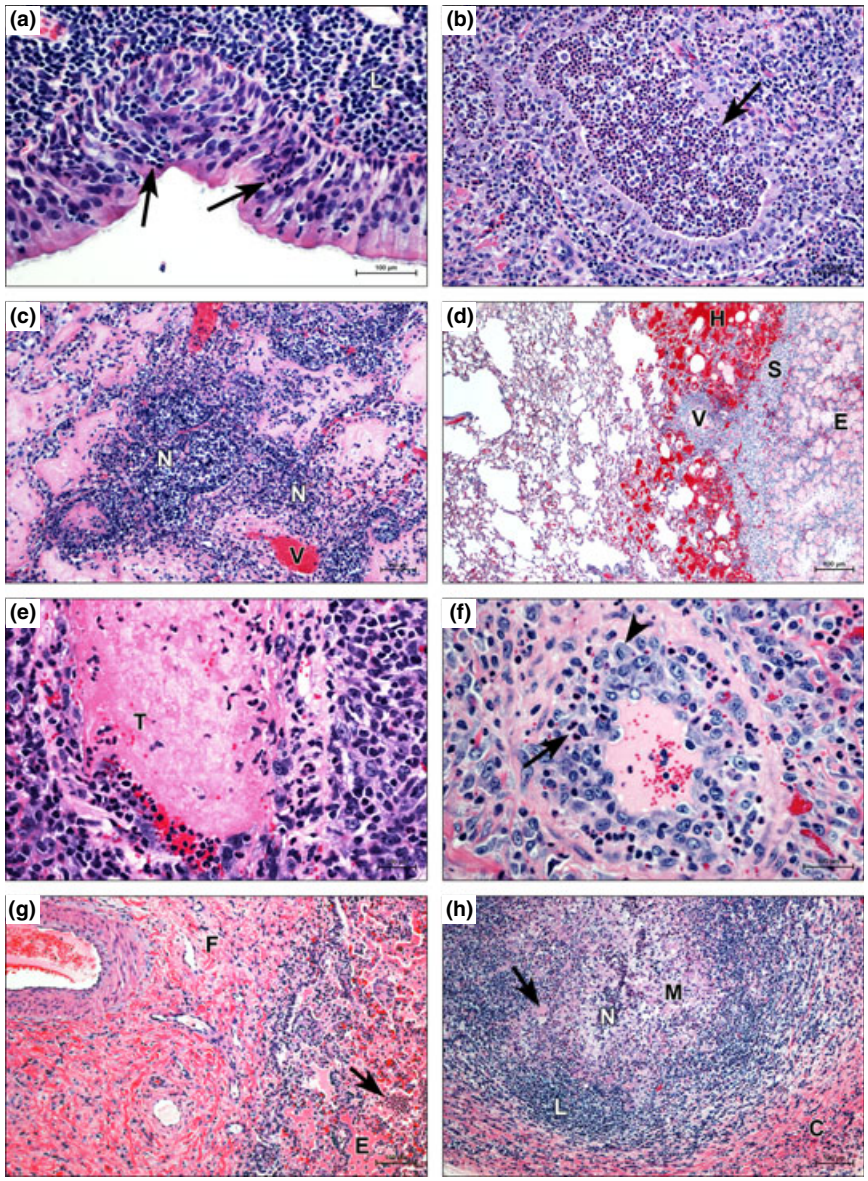

Figure 6 Respiratory lesions of percutaneous caprine melioidosis. (a) Suppurative tracheitis showing neutrophil transcytosis (arrows) and submucosal expansion by a thick band of lymphoplasmacytes (L); (b) suppurative bronchiolitis with focal necrosis of the bronchiolar wall (arrow) and luminal aggregates of neutrophils; (c) early vasocentric abscess formation, neutrophils (N) exiting vessel (V) and filling perivascular alveolar and interalveolar spaces; (d) microscopic pulmonary haemorrhage centreed on interlobular vessel (V), haemorrhage (H) to the left of interlobular septum (S) and oedema (E) to the right; (e) a fibrinocellular thrombus (T) occludes the lumen of a small vein; (f) small arteriole, typical lesion of leukocytoclastic vasculitis with neutrophil infiltration (arrow) into the wall and medial hyperplasia, evidenced by a mitotic figure (arrowhead); (g) chronic active bronchointerstitial pneumonia showing septal fibrosis (F) alongside alveolar oedema (E), and suppurative inflammation (arrow); and (h) pulmonary pyogranuloma encased in a thick fibrous capsule (C), an outer mantle of lymphocytes (L) and an inner core of macrophages (M), including giant cells (arrow), which have effected near complete resolution of the liquefactive centre via phagocytosis of neutrophils (N) and cellular debris. Haematoxylin and eosin staining.

Mediastinal and tracheobronchial LNs. Changes at days 2–7 were typically mild, with only lymphoid hyperplasia and intact neutrophils draining into the node. More advanced changes included prominent lymphoid hyperplasia; capsulitis; subcapsular expansion by oedema, neutrophils and macrophages; and multifocal haemorrhages in the medullary sinuses with mixed inflammation. These lesions were similarly present at day 14, along with the development of pyogranulomas. Later time points revealed either resolution of the suppurative lymphadenitis or the progressive development of pyogranulomas, with or without partial resolution.

Cytokine response

Cytokine analysis was conducted on sera from goats from the current percutaneous study alongside sera from goats from a previous aerosol infection study (Soffler *et al.* 2012). A significant effect of day was found for TGF-β1 in both percutaneously ($P = 0.0005$) and aerosol ($P = 0.0048$)-infected goats, as well as significant effects of route ($P = 0.0016$) and route × day interaction ($P < 0.0001$). There were significant decreases in TGF-β1 from day 0 to day 2 in both groups, but only significant elevation above day 0 at days 14 and 21 in the percutaneous group, with no significant difference from pre-infection levels seen on day 42 (Figure 7a). Significant differences in the aerosol group were primarily composed of elevations at days 7, 14 and 21 over the day 2 trough. The concentration of TGF-β1 was significantly lower in the subcutaneous group on days 0, 2 and 14 when compared to the corresponding days in the aerosol group.

IFNγ showed a significant effect of day in percutaneously ($P = 0.017$), but not aerosol ($P = 0.067$)-infected goats. The significance was a result of the elevation of IFNγ observed on day 42 that was significantly higher than all other time points (Figure 7b).

Given the importance of CCL2 in the early immune response to *B. pseudomallei*, comparisons of day 0 and day 2 were made for both routes of infection, even though the overall effect of day was not significant, aerosol ($P = 0.15$) and percutaneous ($P = 0.56$). This comparison showed a significant increase in CCL2 in aerosol infected ($P = 0.027$), but not percutaneously infected goats ($P = 0.47$) on day 2 (Figure 7c). Comparisons were not made for IFNγ in aerosol-infected goats despite the near significance of effect of day because no similar *a priori* predictions were in place. Cytokine data are summarized in Figure 7, with the exception of IL-10, which did not show any significant changes in response to infection in either group.

Discussion

The routes of inoculation and infecting dose of *B. pseudomallei* have been repeatedly shown to be key determinants of disease kinetics, severity and clinical presentation in experimental animals. These factors almost certainly play similar roles in human disease, but are much more difficult to evaluate as the exposure, dose and time to presentation are unknown. Human clinical presentation is highly variable, ranging from peracute septic shock and death to localized skin infections to chronic pneumonia and visceral abscesses, with suppurative infection of virtually any organ.

Following infection with *B. pseudomallei*, approximately 75% of goats in this study developed fever, in contrast to what was seen previously in goats infected by aerosol, where 100% developed fever and the mean temperature remained in the febrile range for the first 9 days postinfection, not returning to pre-infection temperatures until after day 14 (Soffler *et al.* 2012). The greater variability in fever appears

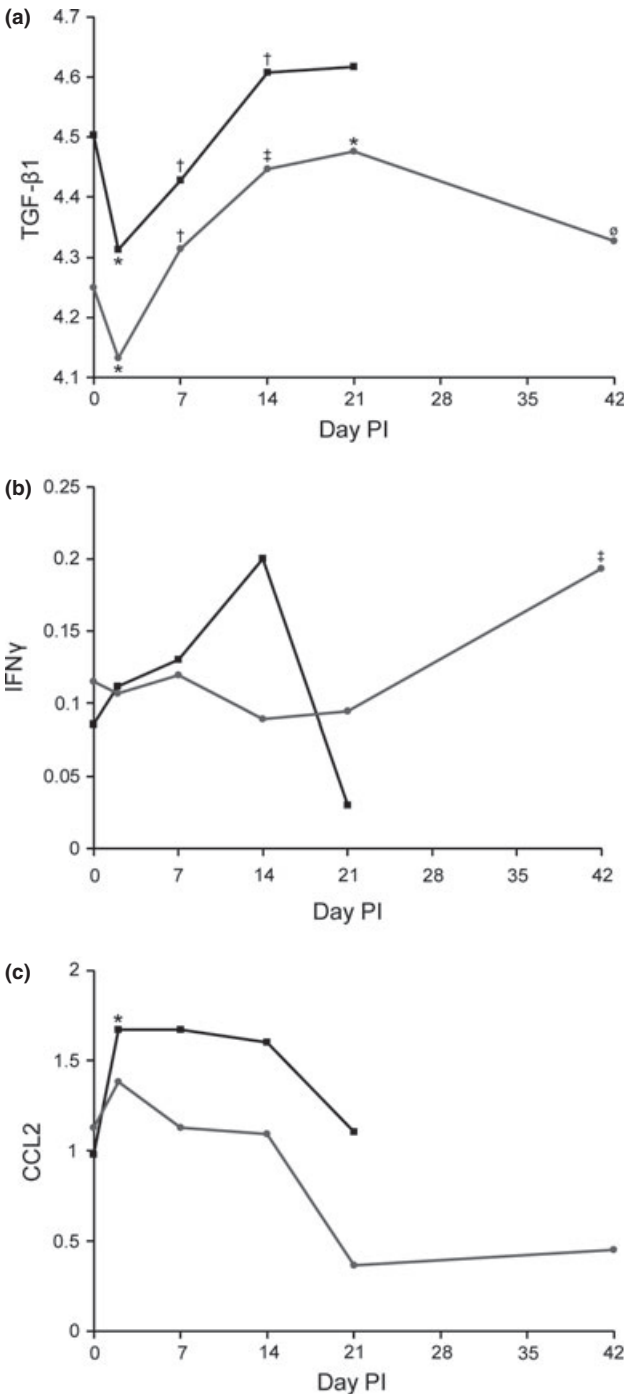

Figure 7 Cytokine production in goats infected with *B. pseudomallei*. Responses of (a) TGF-β1 (log pg/ml), (b) IFNγ (log ng/ml) and (c) CCL2 (log ng/ml) in aerosol (■) and percutaneous (●) groups. Significant elevations were only present for CCL2 in aerosol-infected goats and IFNγ in percutaneously infected goats. TGF-β1 shows an initial decrease followed by increases through day 21 before returning to pre-infection levels on day 42. (‡) Different than previous measure and pre-infection, (†) different than previous measure but no different than pre-infection, (*) different than pre-infection, (ø) not different than previous measure or pre-infection, significance $P < 0.05$.

to be route dependent, where a localized percutaneous inoculum is more easily contained and may reflect individual host factors associated with the immune response compared to widespread pulmonary infection where bacterial factors dominate the initial presentation of infection.

Significant correlations between temperature and granulocyte and lymphocyte counts were seen in goats infected by both percutaneous and aerosol routes [granulocyte ($r = 0.26$, $P = 0.0082$), lymphocyte ($r = -0.20$, $P = 0.037$)]. Neutrophils have been shown to be critical in the host response to *B. pseudomallei* (Easton *et al.* 2007), and acute neutrophilia has been observed in both murine and NHP models (Chin *et al.* 2010; Yeager *et al.* 2012). The importance of the increasing lymphocyte count was evident in the longer percutaneous study (42 *vs.* 21 day aerosol). The defervescence on day 18 matching the onset of lymphocytosis in goats in the current study suggests the development of an adaptive immune response, which was supported by the histologic transition to chronic and/or controlled disease.

Goats appear to be able to mount an efficacious adaptive immune response to *B. pseudomallei*, as evidenced by the presence of sterile lesions in both natural and experimental disease (Olds & Lewis 1954; Laws & Hall 1964; Thomas *et al.* 1988). One sterile lesion was observed, although it did not have the typical dry, crumbly appearance noted in these earlier studies, which appears to be associated with older lesions. The role of the adaptive immune response in disease resolution (but not necessarily susceptibility) has been shown in other experimental models as well as melioidosis patients (Ketheesan *et al.* 2002; Barnes *et al.* 2004; Healey *et al.* 2005; Haque *et al.* 2006).

Pneumonia is the most common presentation of human melioidosis, with just over 50% of patients presenting with primary pneumonia and another 8% having secondary pneumonia (Currie *et al.* 2010). While 100% occurrences of pulmonary lesions in experimental inhalational infection, we expected <50% of goats to develop pulmonary lesions following percutaneous infection as at least a portion of pulmonary presentations in human disease are a result of inhalational infection, which was not a factor in this study. The clear predilection for the respiratory tract observed in this study, such that the rapid development of pulmonary lesions seen following percutaneous infection may confound the diagnosis of a primary pneumonia in human melioidosis patients that is actually secondary to inoculation and haematogenous spread.

The radiographic pattern and distribution of caprine pulmonary lesions in percutaneous melioidosis was similar to the finding in human disease and typically characterized by bronchointerstitial infiltrates and pulmonary nodules, which were more prominent in the dorsal aspect of the caudal lung lobes, consistent with haematogenous dissemination (Muttarak *et al.* 2009). Human patients with radiographic evidence of acute pulmonary melioidosis additionally often show patchy alveolar infiltrates and nodular lesions with rapid radiographic and clinical progression, which is typically fatal (Patterson *et al.* 1967; Bateson & Webling 1981). This was similar to the disease in BpG42, which had moderate patchy bronchointerstitial and alveolar infiltrates and nodules on day 7 and rapidly progressed to diffuse disease and death on day 9.

There were considerable similarities in the appearance of radiographic lesions, as well as gross and microscopic lesions, for the two routes of infection, although percutaneously infected goats typically exhibited less severe disease as judged by the size and number of pulmonary nodules and milder bronchointerstitial infiltrates, but with more vasocentric lesions (Soffler *et al.* 2012). The two notable differences seen in the percutaneously infected goats were the regression of lesions and the development of cavitary lesions, which were likely both a function of a longer study duration. The latter has not been reported in any experimental infection and only once from natural disease in sheep (Lewis & Olds 1952), despite the fact that cavitary lesions are common in human pulmonary melioidosis and similarly appear to be associated with subacute/chronic disease (Everett & Nelson 1975; Ip *et al.* 1995; Lim & Chong 2010).

Marked suppurative inflammation developed subsequent to percutaneous inoculation, which was shortly followed by multi-organ dissemination. The most likely route of dissemination was through draining ectatic lymphatics to the prescapular LN and then through efferent lymphatics to the blood stream. The observed vasculitis at the site of infection could also allow direct haematogenous invasion and dissemination of *B. pseudomallei*.

The association of vasculitis with lesion development strongly supports haematogenous dissemination. Uniformly negative blood cultures, despite the collection of large blood volumes, highlight the low levels and intermittent bacteraemia responsible for dissemination in goats, which is likely similar to human disease where documented bacteraemia is typically found at very low levels in approximately half of patients.

Dissemination of infection was more rapid than observed previously in goats infected by aerosol, which typically did not show extrapulmonary spread before day 14. Additionally, the histologic appearance of lesions was often more severe than the lesions observed following aerosol infection (Soffler *et al.* 2012). Haemorrhage was more frequently observed both directly in tissues and in lymph nodes that were draining areas of haemorrhage following percutaneous infection, whereas haemorrhage was primarily associated with severe, fatal disease after aerosol infection.

The involvement of other extrapulmonary organs was generally similar to that seen in human and other experimental disease models with the exception of gross liver lesions, which has been previously noted (Soffler *et al.* 2012). Splenic capsulitis was common as in the aerosol infection model, with the additional finding of splenic neuritis, which could be a source of the abdominal pain observed in human patients (Dhiensiri & Eua-Ananta 1995; Maude *et al.* 2012). A novel finding in the caprine percutaneous infection model was the presence of microscopic cardiac lesions of interstitial myocarditis. The lesions were highly

consistent, but never severe enough to cause clinical manifestations.

The other highly consistent finding was abscessation of the draining lymph node. This has been found in previous caprine models (Narita *et al.* 1982; Thomas *et al.* 1988), but is only reported in 2% human melioidosis patients (Currie *et al.* 2010). Of the patients with suppurative lymphadenitis, the majority of lymph nodes involved were in the head and neck, with only one report documenting inguinal lymph node involvement (Chlebicki & Tan 2006). A higher incidence of inguinal lymph node involvement would be expected because many rice farmers are believed to be infected percutaneously through cuts on their feet. Natural disease in goats has also been shown to involve lymph nodes, but the most commonly affected are the MedLNs draining the lungs (Olds & Lewis 1954; Laws & Hall 1963; Choy *et al.* 2000). Prescapular lymph nodes (draining the forelimb) have been found to be affected in naturally infected goats as well, but much less frequently (Lewis & Olds 1952; Sutmoller *et al.* 1957; Laws & Hall 1964). This suggests either that percutaneous inoculation is actually an uncommon cause of natural infection or much smaller inocula are involved with natural disease such that significant enlargement and abscessation of the lymph node does not occur.

Early lesions in all organs were dominated by neutrophils, but rapidly progressed to mixed infiltrates mostly composed of macrophages and lymphoplasmacytes and then pyogranulomas with varying degrees of granulation tissue formation and fibrosis. This progression of cell type has also been observed in murine models (Santanirand *et al.* 1999; Lever *et al.* 2009). These early changes were associated with changes in the inflammatory cytokine CCL2, which is typically associated with macrophage infiltration, and significant increases have been observed in acute melioidosis models (*in vitro* and *in vivo*). However, there may be an effect of route, with increases seen in aerosol infection (Laws *et al.* 2011), no significant changes in intranasal infection (Wiersinga *et al.* 2007) and a decrease in transcription following intravenous infection (Chin *et al.* 2010). The effect could be related to bacterial delivery to the pulmonary epithelium, which produces CCL2 in response to *B. pseudomallei* (Sim *et al.* 2009), accounting for the significant increase in CCL2 in only the aerosol-infected goats.

Increases in serum IFNγ are also seen in murine models of acute infection, typically associated with higher organ burdens (Liu *et al.* 2002; Wiersinga *et al.* 2007), as well as in NHP models (Yeager *et al.* 2012). A significant increase in chronic disease (22–45 days PI) has also been shown in a murine model, which was associated with chronic active disease without bacteraemia (Conejero *et al.* 2011). The increase in IFNγ observed in percutaneously infected goats mirrored this finding in chronic disease, although no significant increase in serum IFNγ was observed acutely. This was likely a result of the less acute disease/lower dose at day 2. The elevated serum IFNγ may have also related to the extensive splenic and renal abscessation present in several goats on day 42 and/or the release from inhibition by TGF-β1, which had decreased to pre-infection levels by day 42.

The significance of the observed changes in TGF-β1 is less clear as few studies have examined its role in natural or experimental disease. It is still unclear whether TGF-β1 functions as an anti-inflammatory or pro-inflammatory molecule during infection. TGF-β1 has been shown to be elevated in active cases of human melioidosis and return to normal levels after recovery (Weehuizen *et al.* 2012). The changes observed in goats could be associated with an initial consumption of latent (measured) TGF-β1 and a lag in production, which would explain the day 2 trough (Figure 7a). The subsequent increase corresponded with the period of most active disease followed by a decline at day 42 when disease is more chronic and less active suggesting an immunosuppressive/regulatory role for TGF-β1 in caprine melioidosis.

Elevated IL-10 has been found to be significantly associated with mortality in melioidosis patients, with a 10-fold elevation in non-survivors (Simpson *et al.* 2000). Several murine models (acute and chronic) have not been able to reproduce this finding (Wiersinga *et al.* 2010; van der Windt *et al.* 2010; Conejero *et al.* 2011). One study has demonstrated a significant change in IL-10 over the course of infection, with the largest elevation appearing at day 2 (Laws *et al.* 2011). Significant changes in IL-10 were not observed in the caprine models likely because of the target of subacute to chronic, non-fatal disease.

Throat swabs in human melioidosis patients (the closest approximation for nasal swabs in goats) have a sensitivity of 36% (Wuthiekanun *et al.* 2001), which is very similar to the 35% of goats that were positive by nasal swab in this study. This suggests possible spread of infection between animals, but horizontal transmission is exceedingly rare in human disease (Cheng & Currie 2005). The frequency of positive urine culture in percutaneously infected goats (29%) was also similar to the incidence in human melioidosis (21–23%) (Limmathurotsakul *et al.* 2005; Wuthiekanun *et al.* 2007). The number of bacteria isolated from the urine was quite variable (Table 2) but comparable to quantitative cultures from human patients (Wuthiekanun *et al.* 2007). Positive urine culture was associated with advanced disease in goats, with four of five positive cultures found on day 42 and the fifth positive from the goat with terminal disease, all of which cultured positive from gross renal lesions. This association relates well to the finding that positive urine culture is a negative prognostic indicator in human disease (Limmathurotsakul *et al.* 2005), which could similarly relate to advanced disease.

The strength of a caprine melioidosis model is the ability to compare experimental and natural disease in a species that lives within the endemic range of melioidosis and is epidemiologically similar to humans. The findings presented here provide a detailed clinical, radiographic and pathologic description of the pathogenesis of percutaneous caprine melioidosis, which compares favourably with human disease. The goat appears well suited for the study of subacute

to chronic disease as well as the incorporation of risk factors to model acute human melioidosis.

Acknowledgements

The authors would like to acknowledge Phillip Chapman for consultation on the statistical analysis. This work was supported by NIH/NCRR Ruth L. Kirschstein Institutional NIH T32-RR-007072 and contract AI065357 from NIAID, NIH. Its contents are solely the responsibility of the authors and do not necessarily represent the official views of NIAID or NIH.

References

Barnes J.L., Warner J., Melrose W. *et al.* (2004) Adaptive immunity in melioidosis: a possible role for T cells in determining outcome of infection with *Burkholderia pseudomallei*. *Clin. Immunol.* **113**, 22–28.

Bateson E.M. & Webling D.D. (1981) The radiological appearances of pulmonary melioidosis: a report on twenty-three cases. *Australas. Radiol.* **25**, 239–245.

Brett P.J., Deshazer D., Woods D.E. (1997) Characterization of *Burkholderia pseudomallei* and *Burkholderia pseudomallei*-like strains. *Epidemiol. Infect.* **118**, 137–148.

Cheng A.C. & Currie B.J. (2005) Melioidosis: epidemiology, pathophysiology, and management. *Clin. Microbiol. Rev.* **18**, 383–416.

Cheng A.C., Jacups S.P., Gal D., Mayo M., Currie B.J. (2006) Extreme weather events and environmental contamination are associated with case-clusters of melioidosis in the Northern Territory of Australia. *Int. J. Epidemiol.* **35**, 323–329.

Chin C.Y., Monack D.M., Nathan S. (2010) Genome wide transcriptome profiling of a murine acute melioidosis model reveals new insights into how *Burkholderia pseudomallei* overcomes host innate immunity. *BMC Genomics* **11**, 672.

Chlebicki M.P. & Tan B.H. (2006) Six cases of suppurative lymphadenitis caused by *Burkholderia pseudomallei* infection. *Trans. R. Soc. Trop. Med. Hyg.* **100**, 798–801.

Chou D.W., Chung K.M., Chen C.H., Cheung B.M. (2007) Bacteremic melioidosis in southern Taiwan: clinical characteristics and outcome. *J. Formos. Med. Assoc.* **106**, 1013–1022.

Choy J.L., Mayo M., Janmaat A., Currie B.J. (2000) Animal melioidosis in Australia. *Acta Trop.* **74**, 153–158.

Conejero L., Patel N., de Reynal M. *et al.* (2011) Low-dose exposure of C57BL/6 mice to *Burkholderia pseudomallei* mimics chronic human melioidosis. *Am. J. Pathol.* **179**, 270–280.

Currie B.J. & Jacups S.P. (2003) Intensity of rainfall and severity of melioidosis, Australia. *Emerg. Infect. Dis.* **9**, 1538–1542.

Currie B.J., Ward L., Cheng A.C. (2010) The epidemiology and clinical spectrum of melioidosis: 540 cases from the 20 year Darwin prospective study. *PLoS Negl. Trop. Dis.* **4**, e900.

Dance D.A. (1991) Melioidosis: the tip of the iceberg? *Clin. Microbiol. Rev.* **4**, 52–60.

Dance D.A., King C., Aucken H., Knott C.D., West P.G., Pitt T.L. (1992) An outbreak of melioidosis in imported primates in Britain. *Vet. Rec.* **130**, 525–529.

Dannenberg A.M. Jr & Scott E.M. (1958) Melioidosis: pathogenesis and immunity in mice and hamsters. I. Studies with virulent strains of *Malleomyces pseudomallei*. *J. Exp. Med.* **107**, 153–166.

Dhiensiri T. & Eua-Ananta Y. (1995) Visceral abscess in melioidosis. *J. Med. Assoc. Thai.* **78**, 225–231.

Easton A., Haque A., Chu K., Lukaszewski R., Bancroft G.J. (2007) A critical role for neutrophils in resistance to experimental infection with *Burkholderia pseudomallei*. *J. Infect. Dis.* **195**, 99–107.

Estes D.M., Dow S.W., Schweizer H.P., Torres A.G. (2010) Present and future therapeutic strategies for melioidosis and glanders. *Expert Rev. Anti Infect. Ther.* **8**, 325–338.

Everett E.D. & Nelson R.A. (1975) Pulmonary melioidosis. Observations in thirty-nine cases. *Am. Rev. Respir. Dis.* **112**, 331–340.

Fritz P.E., Miller J.G., Slayter M., Smith T.J. (1986) Naturally occurring melioidosis in a colonized rhesus monkey (*Macaca mulatta*). *Lab. Anim.* **20**, 281–285.

Goodyear A., Bielefeldt-Ohmann H., Schweizer H., Dow S. (2012) Persistent gastric colonization with *Burkholderia pseudomallei* and dissemination from the gastrointestinal tract following mucosal inoculation of mice. *PLoS One* **7**, e37324.

Haque A., Chu K., Easton A. *et al.* (2006) A live experimental vaccine against *Burkholderia pseudomallei* elicits CD4+ T cell-mediated immunity, priming T cells specific for 2 type III secretion system proteins. *J. Infect. Dis.* **194**, 1241–1248.

Healey G.D., Elvin S.J., Morton M., Williamson E.D. (2005) Humoral and cell-mediated adaptive immune responses are required for protection against *Burkholderia pseudomallei* challenge and bacterial clearance postinfection. *Infect. Immun.* **73**, 5945–5951.

Hoppe I., Brenneke B., Rohde M. *et al.* (1999) Characterization of a murine model of melioidosis: comparison of different strains of mice. *Infect. Immun.* **67**, 2891–2900.

Ip M., Osterberg L.G., Chau P.Y., Raffin T.A. (1995) Pulmonary melioidosis. *Chest* **108**, 1420–1424.

Jeddeloh J.A., Fritz D.L., Waag D.M., Hartings J.M., Andrews G.P. (2003) Biodefense-driven murine model of pneumonic melioidosis. *Infect. Immun.* **71**, 584–587.

Kaufmann A.F., Alexander A.D., Allen M.A. *et al.* (1970) Melioidosis in imported non-human primates. *J. Wildl. Dis.* **6**, 211–219.

Ketheesan N., Barnes J.L., Ulett G.C. *et al.* (2002) Demonstration of a cell-mediated immune response in melioidosis. *J. Infect. Dis.* **186**, 286–289.

Ketterer P.J., Webster W.R., Shield J., Arthur R.J., Blackall P.J., Thomas A.D. (1986) Melioidosis in intensive piggeries in south eastern Queensland. *Aust. Vet. J.* **63**, 146–149.

Laws L. & Hall W.T.K. (1963) Melioidosis in animals in north Queensland. 1. Incidence and pathology, with special reference to central nervous system lesions. *Queensland J. Agric. Sci.* **20**, 499–513.

Laws L. & Hall W.T.K. (1964) Melioidosis in animals in North Queensland IV. Epidemiology. *Aust. Vet. J.* **40**, 309–314.

Laws T.R., Simpson A.J.H., Nelson M. (2011) Progression of disease in a more clinically relevant mouse model of respiratory melioidosis. *J. Infect. Dis. Immun.* **3**, 183–188.

Leakey A.K., Ulett G.C., Hirst R.G. (1998) BALB/c and C57Bl/6 mice infected with virulent *Burkholderia pseudomallei* provide contrasting animal models for the acute and chronic forms of human melioidosis. *Microb. Pathog.* **24**, 269–275.

Lever M.S., Nelson M., Stagg A.J., Beedham R.J., Simpson A.J. (2009) Experimental acute respiratory *Burkholderia pseudomallei* infection in BALB/c mice. *Int. J. Exp. Pathol.* **90**, 16–25.

Lewis F.A. & Olds R.J. (1952) Melioidosis in sheep and a goat in North Queensland. *Aust. Vet. J.* **28**, 145–150.

Lim K.S. & Chong V.H. (2010) Radiological manifestations of melioidosis. *Clin. Radiol.* **65**, 66–72.

Limmathurotsakul D., Wuthiekanun V., Chierakul W. *et al.* (2005) Role and significance of quantitative urine cultures in diagnosis of melioidosis. *J. Clin. Microbiol.* **43**, 2274–2276.

Limmathurotsakul D., Wongratanacheewin S., Teerawattanasook N. *et al.* (2010) Increasing incidence of human melioidosis in Northeast Thailand. *Am. J. Trop. Med. Hyg.* **82**, 1113–1117.

Limmathurotsakul D., Thammasart S., Warrasuth N. *et al.* (2012) Melioidosis in animals, Thailand, 2006–2010. *Emerg. Infect. Dis.* **18**, 325–327.

Liu B., Koo G.C., Yap E.H., Chua K.L., Gan Y.H. (2002) Model of differential susceptibility to mucosal *Burkholderia pseudomallei* infection. *Infect. Immun.* **70**, 504–511.

Maude R.R., Vatcharapreechasakul T., Ariyaprasert P. *et al.* (2012) Prospective observational study of the frequency and features of intra-abdominal abscesses in patients with melioidosis in northeast Thailand. *Trans. R. Soc. Trop. Med. Hyg.* **106**, 629–631.

Millan J.M., Mayo M., Gal D., Janmaat A., Currie B.J. (2007) Clinical variation in melioidosis in pigs with clonal infection following possible environmental contamination from bore water. *Vet. J.* **174**, 200–202.

Muttarak M., Peh W.C., Euathrongchit J. *et al.* (2009) Spectrum of imaging findings in melioidosis. *Br. J. Radiol.* **82**, 514–521.

Najdenski H., Kussovski V., Vesselinova A. (2004) Experimental *Burkholderia pseudomallei* infection of pigs. *J. Vet. Med. B Infect. Dis. Vet. Public Health* **51**, 225–230.

Narita M., Loganathan P., Hussein A., Jamaluddin A., Joseph P.G. (1982) Pathological changes in goats experimentally inoculated with *Pseudomonas pseudomallei*. *Natl. Inst. Anim. Health. Q. (Tokyo)* **22**, 170–179.

Nelson M., Dean R.E., Salguero F.J. *et al.* (2011) Development of an acute model of inhalational melioidosis in the common marmoset (*Callithrix jacchus*). *Int. J. Exp. Pathol.* **92**, 428–435.

Olds R.J. & Lewis F.A. (1954) Melioidosis in goats. *Aust. Vet. J.* **30**, 253–261.

Omar A.R. (1963) Pathology of melioidosis in pigs, goats and a horse. *J. Comp. Pathol.* **73**, 359–372.

Patterson M.C., Darling C.L., Blumenthal J.B. (1967) Acute melioidosis in a soldier home from South Vietnam. *JAMA* **200**, 447–451.

Pearson T., U'Ren J.M., Schupp J.M. *et al.* (2007) VNTR analysis of selected outbreaks of *Burkholderia pseudomallei* in Australia. *Infect. Genet. Evol.* **7**, 416–423.

Phuong D.M., Trung T.T., Breitbach K. *et al.* (2008) Clinical and microbiological features of melioidosis in northern Vietnam. *Trans. R. Soc. Trop. Med. Hyg.* **102**(Suppl 1), S30–S36.

Piggott J.A. & Hochholzer L. (1970) Human melioidosis. A histopathologic study of acute and chronic melioidosis. *Arch. Pathol.* **90**, 101–111.

Rammaert B., Beaute J., Borand L. *et al.* (2011) Pulmonary melioidosis in Cambodia: a prospective study. *BMC Infect. Dis.* **11**, 126.

Santanirand P., Harley V.S., Dance D.A., Drasar B.S., Bancroft G.J. (1999) Obligatory role of gamma interferon for host survival in a murine model of infection with *Burkholderia pseudomallei*. *Infect. Immun.* **67**, 3593–3600.

van Schaik E., Tom M., DeVinney R., Woods D.E. (2008) Development of novel animal infection models for the study of acute and chronic *Burkholderia pseudomallei* pulmonary infections. *Microbes Infect.* **10**, 1291–1299.

Sim S.H., Liu Y., Wang D. *et al.* (2009) Innate immune responses of pulmonary epithelial cells to *Burkholderia pseudomallei* infection. *PLoS One* **4**, e7308.

Simpson A.J., Howe P.A., Wuthiekanun V., White N.J. (1999) A comparison of lysis centrifugation, pour plate, and conventional blood culture methods in the diagnosis of septicaemic melioidosis. *J. Clin. Pathol.* **52**, 616–619.

Simpson A.J., Smith M.D., Weverling G.J. *et al.* (2000) Prognostic value of cytokine concentrations (tumor necrosis factor-alpha, interleukin-6, and interleukin-10) and clinical parameters in severe melioidosis. *J. Infect. Dis.* **181**, 621–625.

Soffler C., Bosco-Lauth A.M., Aboellail T.A., Marolf A.J., Bowen R.A. (2012) Development and characterization of a caprine aerosol infection model of melioidosis. *PLoS One* **7**, e43207.

Sprague L.D. & Neubauer H. (2004) Melioidosis in animals: a review on epizootiology, diagnosis and clinical presentation. *J. Vet. Med. B Infect. Dis. Vet. Public Health* **51**, 305–320.

Stanton A.T. & Fletcher W. (1932) *Melioidosis: Studies from the Institute of Medical Research of Federated Malay States*. London: John Bale & Sons and Danielson Ltd.

Suputtamongkol Y., Hall A.J., Dance D.A. *et al.* (1994) The epidemiology of melioidosis in Ubon Ratchatani, northeast Thailand. *Int. J. Epidemiol.* **23**, 1082–1090.

Suputtamongkol Y., Chaowagul W., Chetchotisakd P. *et al.* (1999) Risk factors for melioidosis and bacteremic melioidosis. *Clin. Infect. Dis.* **29**, 408–413.

Sutmoller P., Kraneveld F.C., Van Der Schaaf A. (1957) Melioidosis (Pseudomalleus) in sheep, goats, and pigs on Aruba (Netherland Antilles). *J. Am. Vet. Med. Assoc.* **130**, 415–417.

Tan G.Y., Liu Y., Sivalingam S.P. *et al.* (2008) *Burkholderia pseudomallei* aerosol infection results in differential inflammatory responses in BALB/c and C57Bl/6 mice. *J. Med. Microbiol.* **57**, 508–515.

Thomas A.D., Norton J.H., Forbes-Faulkner J.C., Woodland G. (1981) Melioidosis in an intensive piggery. *Aust. Vet. J.* **57**, 144–145.

Thomas A.D., Forbes-Faulkner J.C., Norton J.H., Trueman K.F. (1988) Clinical and pathological observations on goats experimentally infected with *Pseudomonas pseudomallei*. *Aust. Vet. J.* **65**, 43–46.

Thomas A.D., Forbes-Faulkner J.C., D'Arcy T.L., Norton J.H., Hoffmann D. (1990) Experimental infection of normal and immunosuppressed pigs with *Pseudomonas pseudomallei*. *Aust. Vet. J.* **67**, 43–46.

Van der Lugt J.J., Henton M.M. (1995) Melioidosis in a goat. *J. S. Afr. Vet. Assoc.* **66**, 71–73.

Weehuizen T.A., Wieland C.W., van der Windt G.J. *et al.* (2012) Expression and function of transforming growth factor beta in melioidosis. *Infect. Immun.* **80**, 1853–1857.

Whitmore A., Krishnaswami C.S. (1912) An account of the discovery of a hitherto underscribed infective disease occurring among the population of Rangoon. *Ind. Med. Gaz.* **47**, 262–267.

Wiersinga W.J., Wieland C.W., van der Windt G.J. *et al.* (2007) Endogenous interleukin-18 improves the early antimicrobial host response in severe melioidosis. *Infect. Immun.* **75**, 3739–3746.

Wiersinga W.J., Calandra T., Kager L.M. *et al.* (2010) Expression and function of macrophage migration inhibitory factor (MIF) in melioidosis. *PLoS Negl. Trop. Dis.* **4**, e605.

van der Windt G.J., Wiersinga W.J., Wieland C.W. *et al.* (2010) Osteopontin impairs host defense during established gram-negative sepsis caused by *Burkholderia pseudomallei* (melioidosis). *PLoS Negl. Trop. Dis.* **4**, e806.

Wong K.T., Puthucheary S.D., Vadivelu J. (1995) The histopathology of human melioidosis. *Histopathology* **26**, 51–55.

Woods D.E., Jones A.L., Hill P.J. (1993) Interaction of insulin with *Pseudomonas pseudomallei*. *Infect. Immun.* **61**, 4045–4050.

Wuthiekanun V., Suputtamongkol Y., Simpson A.J., Kanaphun P., White N.J. (2001) Value of throat swab in diagnosis of melioidosis. *J. Clin. Microbiol.* **39**, 3801–3802.

Wuthiekanun V., Limmathurotsakul D., Wongsuvan G. *et al.* (2007) Quantitation of *B. pseudomallei* in clinical samples. *Am. J. Trop. Med. Hyg.* **77**, 812–813.

Yeager J.J., Facemire P., Dabisch P.A. *et al.* (2012) Natural history of inhalation melioidosis in rhesus macaques (*Macaca mulatta*) and African green monkeys (*Chlorocebus aethiops*). *Infect. Immun.* **80**, 3332–3340.

Supporting information

Additional Supporting Information may be found in the online version of this article:

Figure S1. Normal Caprine Thoracic Radiograph